Opto-Electronics Review

journal homepage: https://journals.pan.pl/opelre


# Discussion around IR material and structure issues to go toward high performance small pixel pitch IR HOT FPAs

Olivier Gravrand[1*], Nicolas Baier[1], Alexandre Ferron[1], Florent Rochette[1], Clément Lobre[1], Jocelyn Bertoz[2], Laurent Rubaldo[2]

[1]CEA-LETI, 17 des Martyrs St., 38054 Grenoble, France
[2]Lynred, BP 21, 38113 Veurey-Voroize, France

**Article info**

*Article history:*
Received 15 Oct. 2022
Received in revised form 28 Dec. 2022
Accepted 17 Jan. 2023
Available on-line 16 Mar. 2023

*Keywords*:
Mid-wave infrared; focal plane array; high operating temperature; small pitch; modulation transfer function; finite element method.

**Abstract**

In the last decade, infrared imaging detectors trend has gone for smaller pixels and larger formats. Most of the time, this scaling is carried out at a given total sensitive area for a single focal plane array. As an example, QVGA 30 µm pitch and VGA 15 µm pitch exhibit exactly the same sensitive area. SXGA 10 µm pitch tends to be very similar, as well. This increase in format is beneficial to image resolution. However, this scaling to even smaller pixels raises questions because the pixel size becomes similar to the IR wavelength, but also to the typical transport dimensions in the absorbing material. Hence, maintaining resolution for such small pixel pitches requires a good control of the modulation transfer function and quantum efficiency of the array, while reducing the pixel size. This might not be obtained just by scaling the pixel dimensions. As an example, bulk planar structures suffer from excessive lateral diffusion length inducing pixel-to-pixel cross talk and thus degrading the modulation transfer function. Transport anisotropy in some type II superlattice structures might also be an issue for the diffusion modulation transfer function. On the other side, mesa structures might minimize cross talk by physically separating pixels, but also tend to degrade the quantum efficiency due to a non-negligible pixel fill factor shrinking down the pixel size. This paper discusses those issues, taking into account different material systems and structures, in the perspective of the expected future pixel pitch infrared focal plane arrays.

## 1. Introduction

Decreasing the pixel pitch is today a strong trend in cooled infrared (IR) focal plane arrays (FPA). Since the late 2000s, the standard pixel has switched from 30 µm to 15 µm, staying in the same FPA surface. It resulted in a clear improvement in image resolution, from QVGA to VGA. Since the mid-2010s, a new product line tends to emerge in Europe [1, 3] for microwave (MW) detectors with 10 µm pitch, and today's research focuses on even smaller pixels, 7.5 µm or lower [4, 5]. On the US side, demonstrations of a 5 µm pitch MW array have been made [6, 7] and today a 6 µm pitch HgCdTe (MCT) product is available [8]. A large effort has also been made within the VISTA program targeting Sb-based type II superlattice (T2SL) material system, with numerous 5 µm pitch FPA demonstrations [9].

The motivation for this race for a small pixel has been extensively discussed in the literature [10, 11]. Indeed, pitch reduction is about increasing the resolution of the imager, while keeping the same array area. The final goal is usually to increase the range, whether it is a detection, reconnaissance or even identification range. However, the range is closely related to the minimum resolvable temperature difference (MRTD). This figure of merit (FOM) is usually defined in the first approximation as

$$\mathrm{MRTD} = K\,\frac{\mathrm{NETD}}{\mathrm{MTF}}\,, \tag{1}$$

with $K$ – the system related constant (including optical parameters and others), MTF – the focal plane array

*Corresponding author at: olivier.gravrand@cea.fr

https://doi.org/10.24425/opelre.2023.144561
1896-3757/ Association of Polish Electrical Engineers (SEP) and Polish Academic of Sciences (PAS). Published by PAS

modulation transfer function, and NETD – the noise equivalent temperature difference proportional to the noise and inversely proportional to the quantum efficiency (QE)

$$\mathrm{NETD} \propto \frac{\mathrm{noise}}{\mathrm{QE}}. \tag{2}$$

When dealing with background-limited detectors (BLIP limit), the noise is then proportional to the square roots of the photocurrent so that the noise $\propto F\sqrt{\mathrm{QE}}$ with $F$ being the excess noise factor taking into account potential other noise sources (such as dark current or excessive residual fixed pattern noise). One ends up with the MRTD expressed as

$$\mathrm{MRTD} \propto \frac{F}{\mathrm{MTF} \cdot \sqrt{\mathrm{QE}}}. \tag{3}$$

Therefore, MTF has a strong importance on the final performance in terms of range, but QE and other sources of noise should not be forgotten. In the rest of the paper, the authors will discuss performance using MTF $\cdot \sqrt{\mathrm{QE}}$ so that MTF appears more important than QE. This might be the case of recognition or identification phases, where the flux is large enough. However, in some situations where the flux is low regarding the detector noise, the QE might become more important than MTF. This is the typical situation of detection, occurring first, before recognition or even identification.

To illustrate this, Figure 1 represents this MTF $\cdot \sqrt{\mathrm{QE}}$ *vs*. spatial frequencies for different pitches, from 30 µm down to 5 µm. Dashed lines represent the ideal situation where the pixel has an ideal QE (QE = 1) onto its whole surface: the point spread function (PSF) is square with a width identical to the pitch, and, therefore, the MTF is a sinc function

$$\mathrm{MTF} = |\,\mathrm{sinc}(\pi f\ \mathrm{pitch})\,|. \tag{4}$$

Plain lines, on the other hand, represent the situation where the sensitive surface is smaller than the pixel (d$x$ = 2 µm smaller in size). The result is a decrease in QE due to a decrease in fill factor (FF) – FF = (pitch − d$x$)$^2$/pitch$^2$.

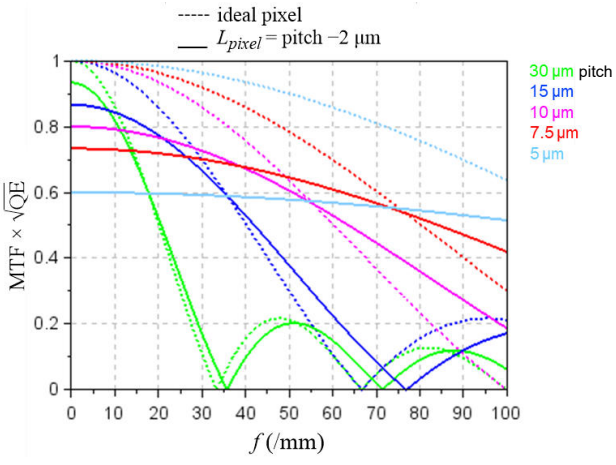


**Fig. 1.** Example of the ideal pixel MTF (dashed lines) and MTF for a pixel smaller than the pitch (solid lines) for different pitches.

Another effect is a slight shift towards the high frequencies of the MTF first zero due to the smaller width of the pixel, so that it can be written as

$$\mathrm{MTF} = \mathrm{FF} \times |\,\mathrm{sinc}(\pi f\ [\mathrm{pitch} - \mathrm{d}x\,])\,|. \tag{5}$$

Of course, pixels as large as 30 µm pixels are not very sensitive to this non ideal FF. However, the curves tend to deviate from the ideal case for small pixels, significantly degrading the performance for 10 µm pixels and smaller. An interesting point to note is that performance at Nyquist frequency is not enough to qualify the performance of the imaging retina. Indeed, looking at 7.5 µm pitch curves for instance, it can be seen that around Nyquist frequency (66 mm$^{-1}$), the MTF $\cdot \sqrt{\mathrm{QE}}$ performance is very similar for the two configurations, but low FF pixel performance exhibits much lower performances for lower frequencies, down to 25% lower.

## 2. Different structures considered for small pixels pitches

Roughly, four kinds of structures are usually considered for small pixel pitch FPAs, and will be discussed here:

1. Planar structures

In this kind of structure, the absorbing layer is not reticulated, and photo-carriers are collected after diffusion. This structure offers a strong advantage: the narrow gap might stay encapsulated during the entire process, so that no process-induced defect affects its performances. It is, for instance, the case of shallow-etched barrier structures: the absorbing layer always stays protected/passivated by the barrier layer. Another advantage is that passivation deposition is usually easier for a planar structure than for a textured structure.

However, planar structures suffer from the fact that diffusion also occurs laterally so that a given carrier generated in front of one collector has a non-negligible probability to be collected by one of the neighbouring pixels, thus enlarging the point spread function (PSF) and degrading the MTF [13].

2. Fully depleted structures

In a planar structure, the collector is a space charge region, generally, from a pn junction. This depletion region might extend into the absorbing layer if the applied bias is strong enough regarding the doping level of the absorbing layer. When photo-generated carrier drifts into the depletion layer, the photo-carrier drifts towards the collector so that it has no chance to be collected elsewhere. When designed properly, such a structure might be optimal for MTF (if no diffusion at all occurs in the structures, i.e., if the structure is fully depleted) [7]. However, to be viable at high temperature, the Shockley-Read-Hall (SRH) recombination must be very low in order to limit depletion dark currents to acceptable values [12]. If the electric field is high enough in this depletion region, impact ionization may also occur, which could degrade signal to noise ratio, but this is unlikely for the thick depletion required for good QE.

3. Mesa structures

In this kind of structure, pixels are fully separated by deep reticulation trenches. Consequently, the MTF is

expected to be perfect. However, this reticulation suffers from different issues. First, the pixel FF.

FF might be degraded by the loss of absorbing material in the trenches. Then, those trenches being usually done by etching planar layers, the mesa walls might be degraded by process-induced defects, thus degrading the stability or even the dark current. Also, the light may enter the trench and propagate over long distances polluting other pixels. Finally, yet importantly, diffraction might occur in the trench down tail. The diffraction light may then be guided into the bottom window common layer and may then pollute other pixels onto long distances.

4. Vertical collection structure, commonly called "loophole" in MCT

This very particular structure consists of a vertical collecting junction around a central vias traversing the absorbing structure. The presence of those vertical collectors through the whole thickness of the absorbing layer tends to impede lateral diffusion of the photo-generated carrier, thus improving MTF. This structure seems very well suited for small pixel pitches. However, it suffers from few technical issues. The vertical collector is usually obtained by etching a vias throughout the narrow gap absorbing layer, then creating an annular diode around it. Therefore, the management of etching-induced defect has to be correctly addressed so that the diode performances (in terms of noise tail for instance) are not degraded. Moreover, this vias induces a central blind in the pixel, i.e., a small loss in QE. Besides, this central blind tends to tailor the theoretical pixel MTF towards a slightly better MTF than the ideal sinc pixel, which is then advantageous for small pixels.

## 3. Focus on the planar structure

In the planar structure, the absorbing layer is not physically reticulated and remains planar. Usually, the reticulation is carried out using localised ion implantation, thus forming localised pn junctions, as represented in Fig. 2. Usually, the absorbing layer is mostly a flat band so that photo-generated carriers must diffuse up to the pixel charge collector, the pn junction space charge region (SCR). This diffusion induces randomness in the collection so that a given carrier has a non-null probability to be collected by its neighbouring pixel, thus enlarging the PSF and degrading the MTF. However, the presence of neighbouring collecting photodiodes plays an important role in the PSF. Indeed, when generated in the absorbing layer, the photo-carrier will investigate the crystal around him, randomly walking during its lifetime (before recombination). If, during the time, it visits a pixel charge collector, it will be immediately collected and will contribute to the photocurrent of this pixel. Therefore, for an isolated diode, the collection probability decreases exponentially with the distance to the diode as can be seen on the measured PSF represented in Fig. 3 bottom plot.

Neglecting interface recombination, the rate of this exponential decrease is a good estimation of the diffusion length $L_d = \sqrt{kT \cdot \mu \cdot \tau}$ in the absorbing material and depends on the lifetime $\tau$ and mobility $\mu$ of the considered minority carrier. However, if the diffusion area contains other collecting diodes, the probability for this photo-

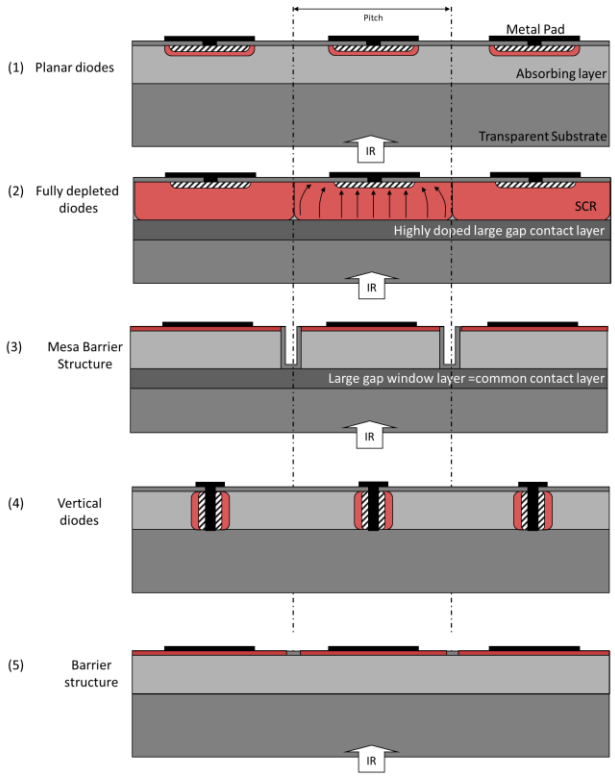


**Fig. 2.** Schematic representation of the different structures discussed.

generated carrier to be collected by the central pixel is the probability that during its lifetime it encounters the central pixel, multiplied by the probability it does not visit the neighbouring diodes during the same time. This gives, therefore, much sharper PSF profiles as may be seen on the PSF mapping shown on the upper plot in Fig. 3. The obtained cloverleaf shape in the PSF is characteristic of a self-confinement of the diffusion within an array of photodiodes and may be computed using semiconductor derivative partial equations as in Ref. 13. Consequently, the resulting MTF is much better for a planar diode within an array of diodes than for the same diode isolated with no neighbouring diodes. Figure 3 shows an example of such an effect measured on a 7.5 µm pitch MCT planar array, for which the PSF was measured with electron beam induced current (EBIC) microscopy [14] and showed an important improvement of the MTF.

Thus, this self-confinement is a powerful tool to optimize planar structures as discussed in Ref. 15. For MTF optimization ([16] and [17]), the main parameters to play with are:

1. diffusion length,
2. surface recombination,
3. diffusion layer thickness,
4. junction geometry,
5. internal grading.

Indeed, when the diffusion length becomes much larger than the characteristic dimensions of the pixel, the MTF tends to be degraded by the fact that carriers are able to diffuse up to the neighbouring pixels. As an example of this effect, Figure 4 shows an example of two 15 µm pitch planar MCT structures with two different diffusion lengths, one lower than the inter-diode distance and another much

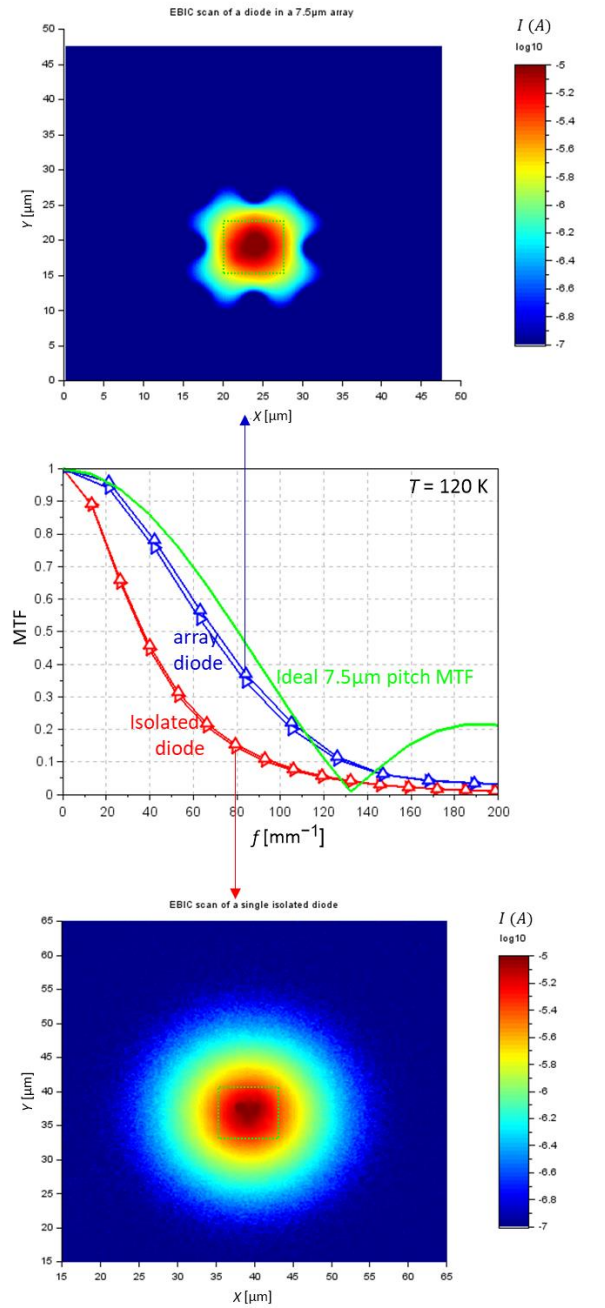


**Fig. 3.** Example of pixel PSF of an isolated MCT diode or inside a 7.5 µm array of neighbouring diodes (EBIC measurement from Ref. 14).

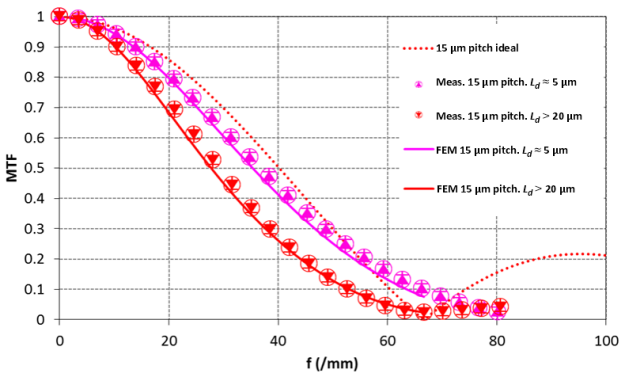


**Fig. 4.** Measured and computed MTF for 15 µm pitch planar MCT diodes, with two different diffusion lengths, from Ref. 15.

higher. As expected, the MTF shows a significant degradation (15% at Nyquist frequency of 33 $mm^{-1}$) with a longer diffusion length.

This MTF limitation by lateral diffusion saturates when diffusion length becomes far larger than the pixel itself as shown in Fig. 5. As can be seen in this plot, a smaller pixel pitch leads to a more degraded MTF if the lateral diffusion is not taken into account in the pixel design.

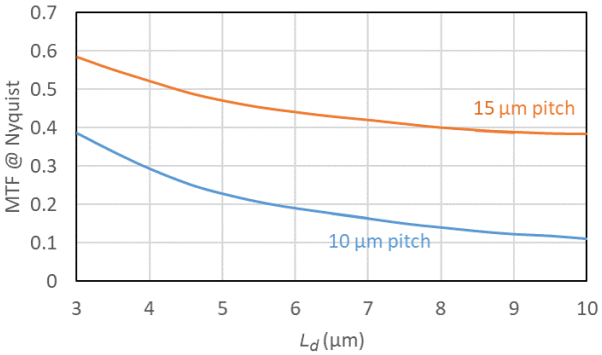


**Fig. 5.** Computation of MTF degradation at Nyquist frequency, due to lateral diffusion for 15 and 10 µm pitch planar MCT diodes, with non-optimized parameters [16].

Besides, for high operating temperature (HOT) detectors, the diffusion limited planar diode must minimize thermal generation of minority carriers into diffusion layer in order to minimize diffusion dark current. In other words, the diffusion layer must have long carrier lifetime, i.e., long diffusion length, which tends to limit the MTF if not properly managed.

Surface recombination velocity sometimes limits the planar diode MTF. Indeed, it induces a shorter effective lateral diffusion, thus optimizing the MTF. Figure 6 shows the computation of the Nyquist frequency MTF as a function of the interface recombination velocities, for 15 and 10 µm pitch planar diodes. The MTF improvement exhibits saturation type curves similar to Fig. 5. This effect is, for instance, quite important in the case of InSb planar diodes as discussed in Ref. 15 where typical interface recombination velocities are in the range of $S \cdot L_d/D = 50$.

The thickness of the diffusion layer is also a very important parameter for the MTF. Indeed, if the carrier is generated close to the collector (the closeness must be understood regarding the diffusion length), the probability

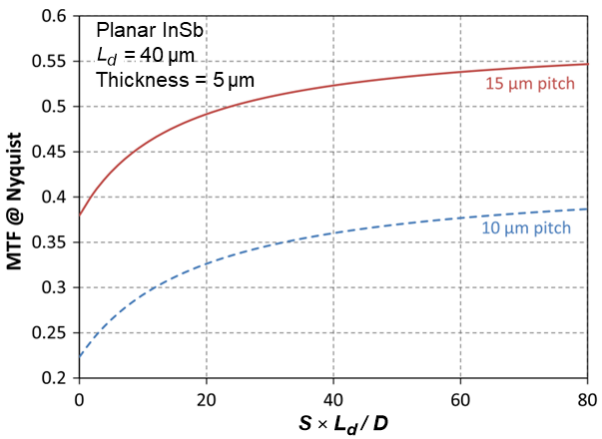


**Fig. 6.** Effect of the surface recombination velocity on planar InSb diodes MTF, from Ref. 15.

for the carrier to visit lateral pixel becomes very low and the MTF is therefore improved. This is illustrated in Fig. 7 for different configurations of 10 µm pitch planar MCT diodes showing a strong improvement of Nyquist MTF from 0.3 up to 0.5 playing solely with the absorbing layer thickness.

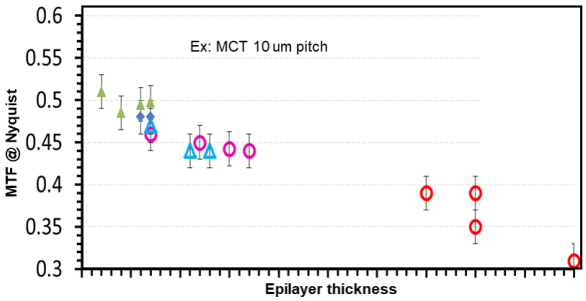


**Fig. 7.** Effect of the epitaxy thickness onto the measured MTF at Nyquist frequency for planar 10 µm pitch MCT diodes, from Ref. 16.

However, absorbing layer thickness is a dangerous parameter to play with as it determines the total optical absorption, i.e., the QE. In other words, decreasing the thickness too much to optimize the MTF will degrade the overall range through the MTF · $\sqrt{\text{QE}}$ parameter.

Other parameters may be used to manage this diffusion MTF. The junction geometry (width and depth) is also a powerful tool to shape the pixel PSF. An example of such optimisation is shown in Fig. 8, which shows the computed MTF of three different configurations of 7.5 µm pitch planar MCT diodes, together with the ideal sinc MTF. The non-optimized planar configuration is given with red dots and exhibits degraded performances: the MTF at Nyquist frequency of 66 mm$^{-1}$ is close to 30% instead of 64% for the ideal case. Counterintuitively, increasing the junction width (i.e., having neighbouring diodes closer to each other) allows a more efficient self-confinement and, thus, a better pixel MTF: the PSF appears much sharper in that case since the neighbouring diodes are also collecting photo-charges. In the case of Fig. 8, a gain of more than 10% in MTF is obtained (purple dots).

Another parameter to be used is the depth of the junction. Figure 8 shows an example of a deep diode (blue dots) with the same width as the standard configuration, but with a much deeper junction. Two effects may be discussed to explain such a gain. First, a deep diode limits the effective diffusion thickness beneath the junction itself, thus optimizing partly the pixel MTF. Second, it appears that the vertical walls give a much sharper contribution to the PSF than the flat horizontal part of the collector. Indeed, the vertical part of the collector is much more efficient in terms of self-confinement than the flat horizontal part. Therefore, the more vertical is this collecting junction; the better will be the pixel MTF. As mentioned previously, deep junctions tend to limit the flat field volume beneath the junction and might, therefore, degrade a bit the QE when the diode is large in the pixel pitch. The ultimate expression of this configuration is the so-called “loophole” structure, where the diodes are indeed fully vertical, located around a contact via fully traversing the absorbing layer. This specific structure will be discussed in section 4.

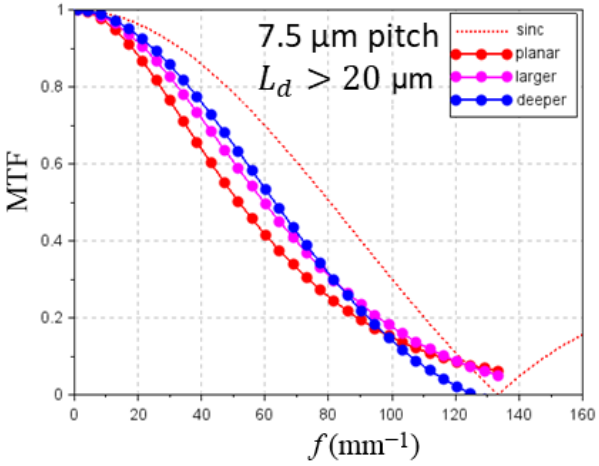


**Fig. 9.** Example of a computed MTF for three different configurations of 7.5 µm planar MCT diodes: standard planar, larger diode, or deeper diode. ($L_d$ >20 µm).

Internal grading may also be used to optimize the planar structure MTF. Indeed, the use of an internal drift is very useful to push the photo-carrier toward the collector in front of it, thus reducing the probability that carrier visits neighbouring pixel by diffusion. Graded doping or graded gap layer are often considered. This optimization option may, however, be handled with care as it may degrade QE or at least the cut-off stiffness of the resulting photodiodes. As an example, Figure 9 shows an example of computed MTF at Nyquist carried out for planar 15 µm pitch MCT diodes with long diffusion length. As expected, the MTF increases as the internal electric field $E/kT$ increases, up to the ideal 64% of the sinc pixel. When the internal field $E$ clearly exceeds $kT$, no diffusion can occur as the structure may be considered as fully depleted.

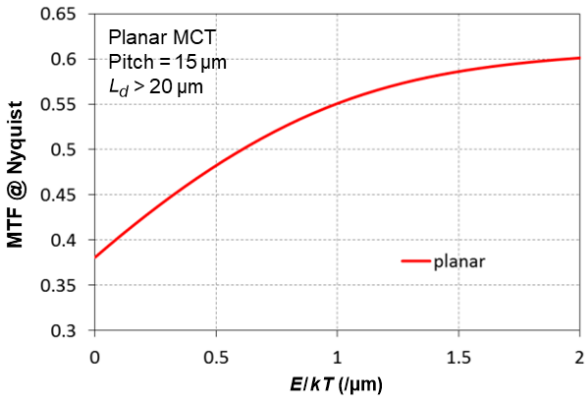


**Fig. 8.** Effect of internal field onto the pixel MTF of a planar MCT diode, from **Błąd! Nie można odnaleźć źródła odwołania.**

At the end, the fully depleted structure, as demonstrated by Teledyne with MCT [7, 18] may look like an ideal planar structure concerning the MTF. In such a structure, the narrow gap is entirely depleted so that no lateral diffusion occurs at all. The price to pay, however, is manifold. The absorbing layer doping may be sufficiently lowered in order to deplete the required thickness for QE. Such a management of a very low residual doping is certainly a challenge for every material system. At the end, the operation of such fully depleted structure at high temperature requires a very high SRH lifetime, in the ms range. Such level of low recombination is claimed by Ref. 18 for MCT but remains under discussion [12].

## 4. The particular case of the vertical junction

The ultimate depth for a planar diode is a structure where diodes become vertical, traversing the entire absorbing layer. This kind of structure has been, for instance, exploited with MCT to fabricate very small pitch arrays, commercially available by Leonardo [6]. In such kind of structure, traversing vias are etched trough the absorbing layer, and pn junctions are formed around those vias in a such way that the charge collectors are totally vertical, thus improving the array self-confinement.

In such a configuration, however, the central part of the pixel becomes blind, which shapes differently the pixel MTF. For a cylindrical configuration with the central blind diameter $w_o$, the ideal MTF becomes

$$\mathrm{MTF}(f) = \mathrm{sinc}\left(\pi f \left[\frac{\mathrm{pitch} - w_o}{2}\right]\right) \times 2\cos(2\pi f x_o),$$

where

$$x_o = \frac{w_o}{2} + \frac{\mathrm{pitch} - w_o}{4} = \frac{\mathrm{pitch}}{4} + \frac{w_o}{2}.$$

The resulting MTF is shown in Fig. 10, for a 7.5 µm pitch with two blind diameters 1 µm or 2 µm. It can be seen that this central blind tends to shift the first zero of the MTF to a shorter frequency, which tends to slightly degrade the MTF (for instance from 132/mm, this value becomes 117/mm with a 1 µm wind central blind). The loss in QE is also visible but not dramatic: the central blindness does not occupy a large part of the pixel area.

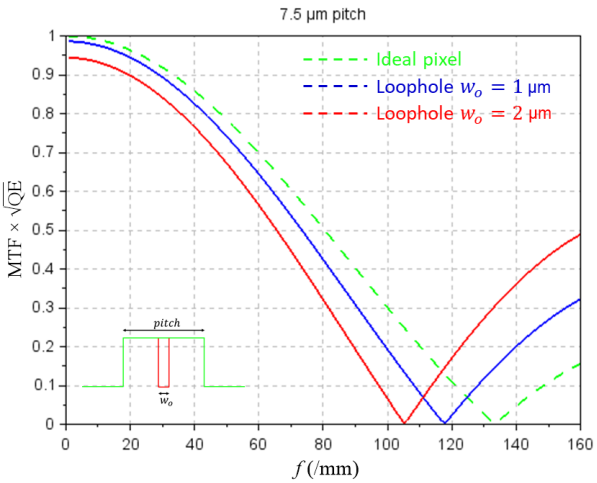


**Fig. 12.** Theoretical MTF for a vertical cylindrical junction at a 7.5 µm pitch, for two central blind geometries.

## 5. Focus on the mesa structure

One very efficient solution for MTF optimization would be to physically separate the pixels with an appropriate mesa etch. To be effective for MTF improvement, the full diffusion layer must be etched. Indeed, for a flip-chip bounded chip, the incoming light usually comes from the rear interface, with an exponential photo-generation (Beer-Lambert law). Most of the photons are absorbed just beneath the rear interface of the diffusion layer, opposite side from the collector. In order to be efficient, the pixel separation has to be etched down to this rear interface, where the photo-generation mainly occurs. For partially etched layers, the MTF might clearly not be optimized, as shown in Fig. 11 illustrating computed MTF for different mesa depth ($H_{\mathrm{mesa}}$) with a given 5 µm MCT layer thickness, taken from Ref. 15.

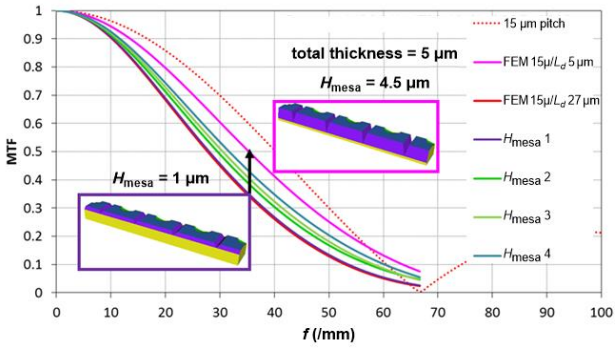


**Fig. 10.** Finite element modelling computation of the MTF degradation of partial mesa etch mesa pixel in MCT, from Ref. 15.

The sensitive area of the pixel being smaller than the pixel itself, the first zero of the MTF shifts toward higher frequencies, and MTF might become better than for an ideal pixel. However, as mentioned previously in this paper (section 3), deep mesas might also induce a loss in FF inducing a rapid degradation of the QE when decreasing the pixel pitch (the trench area goes as the perimeter, which rapidly dominates decreasing the geometry). Therefore, mesa reticulation demands a very high aspect ratio in order not to degrade too much the diode QE. As an example, Figure 12 shows the expected MTF · $\sqrt{\mathrm{QE}}$ for 1 µm wide deep trenches used with different pixel pitches. Typically, small pixel induces a loss of performance at small frequencies, but not much at higher frequencies. In such a case, limiting the analysis simply to the Nyquist frequency might hide a loss in the overall performance. In this example of Fig. 12, a 5 µm pitch MTF is very similar to the ideal pixel value at Nyquist frequency (66/mm) while the low frequency MTF exhibits a 20% loss in performance.

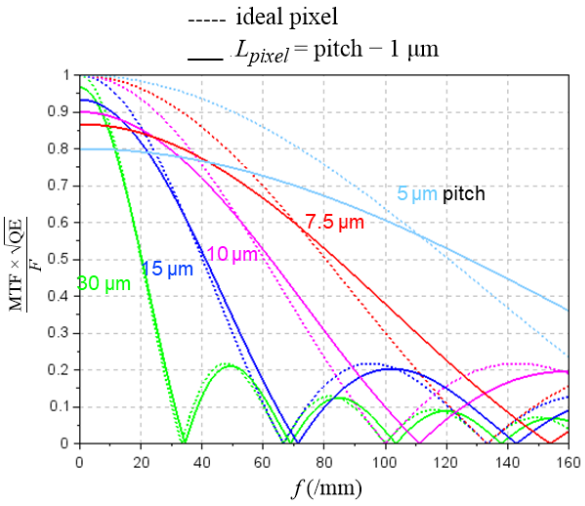


**Fig. 11.** Example of degradation of the MTF · $\sqrt{\mathrm{QE}}$ metric for different pixel pitch with 1 µm wide trenches deep mesa structures. (Dotted lines are ideal sinc pixels and solid lines stand for deep mesa pixels).

Fortunately, this FF loss holds for deep mesa with very steep mesa walls (i.e., flat trench bottom). When the mesa wall is not vertical, the light can reflect onto mesa walls and stay confined into the pixel [19]. The resulting FF loss is lower.

However, other effect may degrade the mesa structure MTF. Indeed, the mesa walls and/trench bottom may diffract incoming light outside its incidence cone, leading to crosstalk between pixels. This has been observed, for instance, in an MCT dual band array with a 30 µm pitch, as shown in Fig. 13, reported in Ref. 19. Light may also propagate over long distances in the trench space itself once again degrading the image quality.

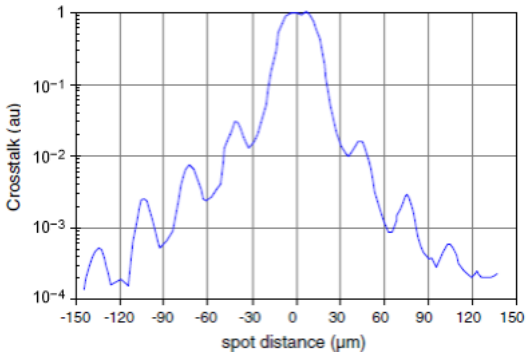


**Fig. 13.** Example of crosstalk degradation induced by diffraction in MCT mesa structures [19].

## 6. The particular case of the barrier structure

Barrier structures (also called nBn [20] or XBn [21]) are formed of a narrow gap layer, covered with a larger gap barrier layer and a contact layer. The hetero structure is designed to allow the transport of minority carriers through the barrier up to the contact layer but limiting the formation of a space charge region into the narrow gap (and, therefore, limiting generation-recombination (GR) dark current). This structure is mainly used for III-V materials (InAsSb- or even Sb-based T2SL), but demonstration has also been done using MCT [22]. Such barrier structure is often used in a shallow etch configuration: only the contact layer is reticulated, so that no damage is done onto the narrow gap material. In this configuration, the barrier layer is acting as an optimal passivation layer for the sensitive layer, which is very convenient.

From a functional point of view, this structure is a planar structure, and is affected by MTF degradation with lateral diffusion. However, the collector here is not a pn junction by the barrier itself, located at the upper surface of the structure, with no possibility to play with the depth of the collector to optimize the pixel MTF.

Another option to manage pixel MTF is to switch from shallow etch to deep mesa configuration to physically separate pixels. However, besides the FF loss, etching this deep mesa might induce defects in the sensitive material, potentially degrading pixel performances in terms of dark, noise, and stability. In other words, the strong benefits of shallow etch are lost and one has to deal with the mesa wall passivation.

Considering the shallow etch, as mentioned previously, an important parameter influencing the pixel MTF is the layer thickness. As an example, Figure 14 shows Nyquist MTF estimations *vs*. diffusion layer thickness (*th*), for 7.5 µm pitch pixels and $\alpha^{-1} = 1$ µm. Different diffusion lengths are represented, smaller than the pixel pitch (3 and 5 µm), as well as larger than the pixel pitch (10 µm). Those computations have been carried out using FEM described in Ref. 15 for an isotropic bulk material and a circular collector located on top of the absorbing layer, and no interface recombination is considered. Clearly, thinning the absorbing layer appears very efficient: the computed MTF remains close to 40% for a 2 µm thickness, even with a 10 µm diffusion length.

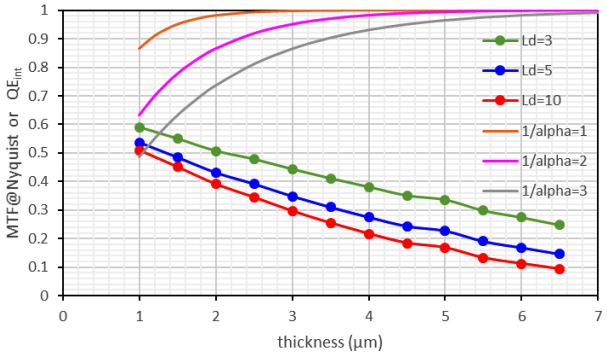


**Fig. 14.** Evolution of barrier device Nyquist MTF *vs*. diffusion layer thickness, for different diffusion lengths $L_d$ (symbols). Optical absorption is also represented for different absorption coefficients.

However, QE might strongly be affected if material is not absorbing enough. In order to quantify this QE loss, the estimated total absorption is also represented in plain lines in Fig. 14, computed as $QE_{int} = [1 - e^{-\alpha \cdot 2\,th}]$ for a two-pass absorption. Different absorptions are considered (expressed as penetration depth $\alpha^{-1}$ in µm). As can be seen, if material is not absorbing enough, the QE loss evolves exponentially with thickness and several tens of % of QE are easily lost. For instance, a penetration depth $\alpha^{-1} = 3$ µm in a 2 µm thick material induces a 25% QE loss, even with the second pass following rear interface reflection in a hybrid configuration. Note that this penetration depth increases when increasing the wavelength up to the peak wavelength of the photodiode or even up to the cut-off. Therefore, the spectral shape will end up smoother for thin layers, even contracting the mid response effective cut-off wavelength toward smaller wavelengths.

The use of a smaller diffusion length (i.e., higher doping) may improve a little bit the situation. Indeed, the MTF is expected to efficiently improve for diffusion smaller than the typical inter-pixel space, as shown in Fig. 15 computed for the same geometry as Fig. 14. This figure also shows that with large diffusion lengths (above 10 µm in this case), the computed MTF saturates. The MTF degradation by diffusion does not change much between 20 and 10 m. Hence, MTF degradation mitigation is only efficient for very short diffusion lengths. For a classical bulk material, the way to shorten diffusion length is to degrade the bulk minority carrier lifetime, usually increasing the doping in the absorbing layer. This can have a significant impact on both the dark current at high temperature (if diffusion limited) but also onto the reachable QE (short diffusion length imposes thin layer and, thus, low absorption).

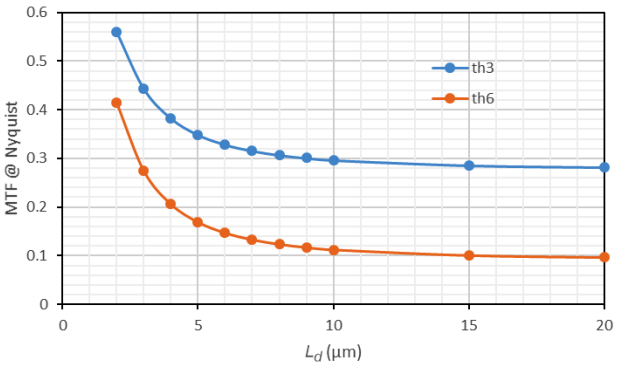


**Fig. 16.** Evolution of computed Nyquist MTF *vs*. diffusion length for barrier device with two different diffusion thicknesses of 3 and 6 µm ($\alpha^{-1} = 1$µm).

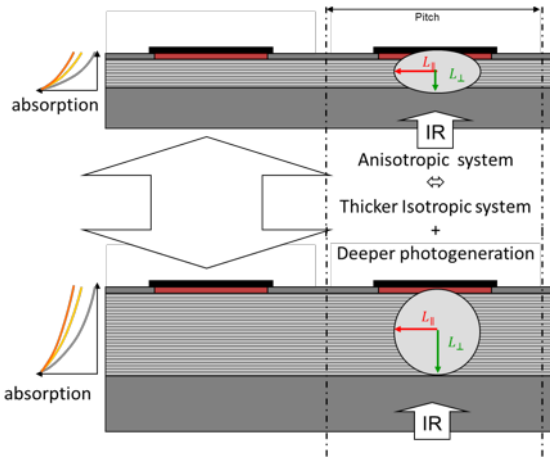


**Fig. 15.** T2SL anisotropic materials are strictly equivalent (from the diffusion point of view) to a thicker layer with a lower absorbing coefficient.

## 7. T2SL particularities

Sb-based T2SL is today an important material system in IR detection as it offers a bulk-like absorption (as opposed to QWIPs) with the ability to easily tailor the material cut-off using super-lattice stack thicknesses. Nowadays, T2SL is most of the time used in barrier configuration in order to limit GR currents.

However, this material system tends to suffer from transport issues: when doped with N, the material is usually highly anisotropic, (see [23] for an example of Ga-based T2SL and [24] for another example of Ga-free T2SL). Due to the superlattice band structure, the transverse mobility is usually much larger than the normal one. This means, in other words, that the diffusion length $L_\perp$ in the vertical direction, perpendicular to the layer plane is much shorter than the in-plane diffusion length $L_\parallel$. Other than QE issues due to an uncompleted collection of photo-generated carriers, this short $L_\perp$ diffusion length might have another deleterious impact on the focal array performance. Indeed, from a diffusion point of view, such an anisotropic material is strictly equivalent to a thicker isotropic material with a deeper optical absorption, as was illustrated in Fig. 16. The effect of diffusion onto the pixel MTF may then be computed using the same tools as previously for isotropic bulk materials. Therefore, such an anisotropy may have strong consequences in terms of MTF for planar barrier structures: one gets the MTF degradation of a thicker layer, which is really not optimal. Note that p-type T2SL is, on the other hand, quite isotropic, as discussed in Ref. 25: this anisotropy concerns mainly the hole bands, not much the electron band. In this context, the key factor is the anisotropic ratio (AR), i.e., the ratio between the in-plane and the vertical diffusion lengths, defined as

$$\mathrm{AR} = \frac{L_\parallel}{L_\perp}.$$

To quantify a bit the effect of this anisotropy onto the pixel MTF, FEM computations have been carried out for a 7.5 µm planar barrier device with

- $L_\parallel = 5$ µm in-plane diffusion length,
- $\alpha^{-1} = 2$ µm optical penetration depth,
- $th = 2$ µm absorbing layer thickness,
- and an anisotropic ratio AR = 3.

Note that this value of the anisotropic ratio is very optimistic as some references are talking about much higher values. As an example, Reference 26 announces a ratio of 400 onto mobilities, i.e., a ratio of 20 onto diffusion lengths.

The resulting MTFs are given in Fig. 17, gathering ideal square pixel in a dotted line, and two distinct computations. The first curve (plain symbols) gives the resulting MTF for the isotropic configuration AR = 1. The second curve (hollow symbols) gives the computed MTF in the anisotropic configuration AR = 3 (emulated with a thicker layer $th = 6$ µm and a deeper absorption $\alpha^{-1} = 6$ µm).

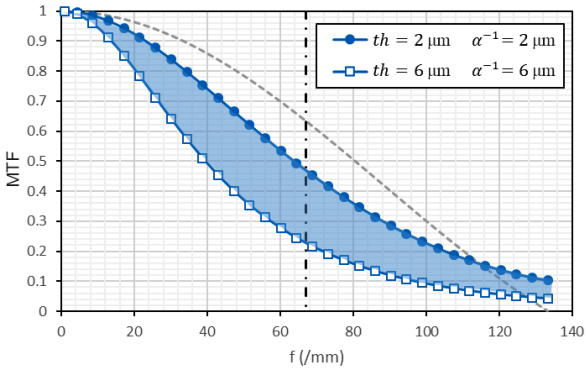


**Fig. 17.** Computation of the effect of anisotropy on the MTF of a 7.5 µm pitch planar barrier pixel, with $L_d = 5$ µm and thickness $th = 2$ µm. AR = 3 is emulated with a factor 3 on thickness $th$ and penetration depth $\alpha^{-1}$.

Looking at the Nyquist frequency, the isotropic configuration gives a 48% MTF (where the ideal pixel value is 64%) which is tolerable for many optical systems. By introducing anisotropy, this value lowers down to 23%, which represents this time a very strong performance degradation.

Integrating the whole MTF from the low frequency to the sampling frequency 1/pitch = 133/mm gives an idea of the total performance degradation. This performance metric is less frightening as both low and high frequencies are less affected by the degradation. In the full band integrated MTF metric, the anisotropy induces 30% loss of performance (shade area in Fig. 17). That kind of effect has already been experimentally observed on even large pixel pitches [27].

For even larger anisotropy, the MTF degradation is even much worse, as Nyquist MTF of 10% and lower can be obtained for AR = 6. Moreover, very large anisotropies imply very short diffusion lengths in the vertical axis, raising other issues concerning QE due to the bad carrier collection of the structure, which will not be discussed here.

## 8. Conclusions

As a conclusion, planar diode or shallow etch barrier structures are very convenient from the processing point of view, but lateral diffusion might degrade MTF performances. In particular, HOT detectors usually imply large carrier lifetimes for low dark current. The resulting large diffusion length is then very disadvantageous for MTF in those arrays. MTF optimization is, however, possible playing with diodes geometry. Thinner layers or internal gradings surely help for MTF but tend to degrade dark current or spectral shape.

However, a high MTF for small planar pixels has already been experimentally demonstrated with a proper optimization of a planar structure using MCT [14].

This MTF degradation due to lateral diffusion is much worst for anisotropic material such as N-type T2SL. Regarding diffusion, an anisotropic material is strictly equivalent to a thicker layer (with a deeper absorption), which is very detrimental for MTF.

Deep mesa delineation is a radical option, but diffusion layer must be fully etched to effectively fight against lateral diffusion. Then, going to very small pitches is an issue: the etching process requires very high aspect ratios to limit FF loss and maintain QE, especially for small pitches. Moreover, this narrow gap etching step usually represents a risk in terms of process-induced crystal defects. Those defects might degrade noise performance and image quality. This etching also raises the need for an efficient mesa wall passivation. Moreover, such mesa structures sometimes exhibit diffraction effects, degrading the crosstalk and, thus, the image quality [19].

## References


[1] Lefoul, X. *et al*. New SOFRADIR 10µm pixel pitch infrared products. *Proc. SPIE* **9249**, 924911 (2014). https://doi.org/10.1117/12.2069254

[2] Lutz, H. *et al*. Ultra-compact high-performance MCT MWIR engine. *Proc. SPIE* **10177**, 101771A (2017). https://doi.org/10.1117/12.2262361

[3] Shkedy, L. *et al*. Development of 10µm pitch XBn detector for low SWaP MWIR applications. *Proc. SPIE* **9819**, 98191D (2016). https://doi.org/10.1117/12.2220395

[4] Gravrand O. *et al*. Design of a small pitch (7.5µm) MWIR HgCdTe array operating at high temperature (130K) with high imaging performances. *Proc. SPIE* **12107**, 121070U (2022). https://doi.org/10.1117/12.2618852

[5] Jeckells, D., Mcewen, R. K., Bains, S. & Herbert, M. Further developments of 8 µ m pitch MCT pixels at Finmeccanica (formerly Selex ES). *Proc. SPIE* **9819**, 98191X (2016). https://doi.org/10.1117/12.2223019

[6] Armstrong, J. M., Skokan, M. R., Kinch, M. & Luttmer, J. D. HDVIP five-micron pitch HgCdTe focal plane arrays. *Proc. SPIE* **9070**, 907033 (2014). https://doi.org/10.1117/12.2053286

[7] Tennant, W. E. *et al*. Small-pitch HgCdTe photodetectors. *J. Electron. Mater*. **43**, 3041–3046 (2014). https://doi.org/10.1007/s11664-014-3192-4

[8] Shafer T. *et al*. High operating temperature (HOT) midwave infrared (MWIR) 6 µm pitch camera core performance and maturity. *Proc. SPIE* **12107**, 121070V (2022). https://doi.org/10.1117/12.2618719

[9] Hill, C. J. *et al*. The VISTA industrial consortium: structure and accomplishments of a government-industry development partnership. *Proc. SPIE* **12107**, 121070P (2022). https://doi.org/10.1117/12.2618983

[10] Kinch, M. The rationale for ultra-small pitch IR systems. *Proc. SPIE* **9070**, 907032 (2014). https://doi.org/10.1117/12.2051335

[11] Holst, G. & Driggers, R. Small detectors in infrared system design. *Opt. Eng*. **51**, 096401 (2012). https://doi.org/10.1117/1.OE.51.9.096401

[12] Gravrand, O. *et al*. Shockley–Read–Hall lifetime study and implication in HgCdTe photodiodes for IR detection. *J. Electron. Mater*. **47**, 5680–5690 (2018). https://doi.org/10.1007/s11664-018-6557-2

[13] Gravrand, O., Desplanches, J. C., Delbegue, C., Mathieu, G. & Rothman, J. Study of the spatial response of reduced pitch HgCdTe dual-band detector arrays. *J. Electron. Mater.* **35**, 1159–1165 (2006). https://doi.org/10.1007/s11664-006-0236-4

[14] Yèche, A. *et al*. MTF characterization of small pixel pitch IR cooled photodiodes using EBIC. *J. Electron. Mater.* **49**, 6900–6907 (2020). https://doi.org/10.1007/s11664-020-08253-0

[15] Gravrand, O. *et al*. MTF Issues in small-pixel-pitch planar quantum IR detectors. *J. Electron. Mater.* **43**, 3025–3032 (2014). https://doi.org/10.1007/s11664-014-3185-3

[16] Berthoz, J. Caractérisation et modélisation par éléments finis des performances des détecteurs infra-rouge refroidis à petits pas. (Université Grenoble Alpes, 2016). (in French)

[17] Pinkie, B. & Bellotti, E. Numerical simulation of the modulation transfer function in HgCdTe detector arrays. *J. Electron. Mater.* **43**, 2864–2873 (2014). https://doi.org/10.1007/s11664-014-3134-1

[18] Lee, D. L. *et al*. Law 19: The ultimate photodiode performance metric. *Proc. SPIE* **11407**, 114070X (2020). https://doi.org/10.1117/12.2564902

[19] Gravrand, O. & Gidon, S. Electromagnetic modeling of n-on-p HgCdTe back-illuminated infrared photodiode response. *J. Electron. Mater.* **37**, 1205–1211 (2008). https://doi.org/10.1007/s11664-008-0478-4

[20] Maimon, S. & Wicks, G. W. nBn detector, an infrared detector with reduced dark current and higher operating temperature. *Appl. Phys. Lett.* **89**, 151109 (2006). https://doi.org/10.1063/1.2360235

[21] Klipstein, P. XBn barrier photodetectors based on InAsSb with high operating temperatures. *Opt. Eng*. **50**, 061002 (2011). https://doi.org/10.1117/1.3572149

[22] Gravrand, O., Boulard, F., Ferron, A., Ballet, P. & Hassis, W. A new nBn IR detection concept using HgCdTe material. *J. Electron. Mater.* **44**, 3069 (2015). https://doi.org/10.1007/s11664-015-3821-6

[23] Ting, D., Soibel, A., Höglund, L. & Gunapala, S. D. Theoretical aspects of minority carrier extraction in unipolar barrier infrared detectors. *J. Electron. Mater.* **44**, 3036–3043 (2015). https://doi.org/10.1007/s11664-015-3756-y

[24] Ting, D., Soibel, A. & Gunapala, S. Type-II superlattice hole effective masses. *Infrared Phys. Technol.* **84**, 102–106 (2017). https://doi.org/10.1016/j.infrared.2016.10.014

[25] Klipstein, P. C. Minority carrier lifetime and diffusion length in type II superlattice barrier devices. *Infrared Phys. Technol.* **96**, 155–162 (2019). https://doi.org/10.1016/j.infrared.2018.11.022

[26] Arounassalame, V. *et al.* Anisotropic transport investigation through different etching depths in InAs/InAsSb T2SL barrier midwave infrared detector. *Infrared Phys. Technol.* **126**, 104315 (2022). https://doi.org/10.1016/j.infrared.2022.104315

[27] Rafol, S. *et al.* Modulation transfer function measurements of type-II mid- wavelength and long-wavelength infrared superlattice focal plane arrays. *Infrared Phys. Technol.* **96** 251–261 (2019). https://doi.org/10.1016/j.infrared.2018.11.006